

Fast Minimum-norm Adversarial Attacks through Adaptive Norm Constraints

Maura Pintor^{1,2} Fabio Roli^{1,2} Wieland Brendel³ Battista Biggio^{1,2}

Abstract

Evaluating adversarial robustness amounts to finding the minimum perturbation needed to have an input sample misclassified. The inherent complexity of the underlying optimization requires current gradient-based attacks to be carefully tuned, initialized, and possibly executed for many computationally-demanding iterations, even if specialized to a given perturbation model. In this work, we overcome these limitations by proposing a fast minimum-norm (FMN) attack that works with different ℓ_p -norm perturbation models ($p = 0, 1, 2, \infty$), is robust to hyperparameter choices, does not require adversarial starting points, and converges within few lightweight steps. It works by iteratively finding the sample misclassified with maximum confidence within an ℓ_p -norm constraint of size ϵ , while adapting ϵ to minimize the distance of the current sample to the decision boundary. Extensive experiments show that FMN significantly outperforms existing attacks in terms of convergence speed and computation time, while reporting comparable or even smaller perturbation sizes.

1. Introduction

Learning algorithms are vulnerable to adversarial examples, i.e., intentionally-perturbed inputs aimed to mislead classification at test time (Szegedy et al., 2014; Biggio et al., 2013). While adversarial examples have received much attention, evaluating the robustness of deep networks against them remains a challenge. Adversarial attacks solve a non-convex optimization problem and are thus prone to finding suboptimal solutions. In particular, all attacks make certain assumptions about the underlying geometry and properties of the optimization problem which, if violated, can derail the attack and may lead to premature conclusions regarding model robustness. That is why the vast majority of defenses published in recent years have later shown to be ineffective against more powerful white-box attacks (Carlini & Wagner,

2017; Athalye et al., 2018). Having an arsenal of diverse attacks that can be adapted to specific defenses is one of the most promising avenues for increasing confidence in white-box robustness evaluations (Carlini et al., 2019; Tramer et al., 2020). While it may seem that the number of attacks is already large, most of them are just small variations of the same technique, make similar assumptions about the optimization problem and thus tend to fail jointly.

In this work, we focus on *minimum-norm* attacks for evaluating adversarial robustness, i.e., attacks that aim to mislead classification by finding the smallest input perturbation according to a given norm. In contrast to *maximum-confidence* attacks, which maximize confidence in a wrong class within a given perturbation budget, the former are better suited to evaluate adversarial robustness as one can compute the accuracy of a classifier under attack for any perturbation budget without re-running the attack. Within the class of gradient-based minimum-norm attacks, there are three main sub-categories: (i) soft-constraint attacks, (ii) boundary attacks and (iii) projected-gradient attacks. Soft-constraint attacks like CW (Carlini & Wagner, 2017) optimize a trade-off between confidence of the misclassified samples and perturbation size. This class of attacks needs a sample-wise tuning of the trade-off hyperparameter to find the smallest possible perturbation, thus requiring many steps to converge. Boundary attacks like BB (Brendel et al., 2019) or FAB (Croce & Hein, 2020b) move along the decision boundary towards the closest point to the input sample. These attacks converge within relatively few steps and are robust to hyperparameter choices, but may require an adversarial starting point and need to solve a relatively expensive optimization problem in each step. Finally, recent minimum-norm projected-gradient attacks like DDN (Rony et al., 2019) perform a maximum-confidence attack in each step under a given perturbation budget ϵ , while iteratively adjusting ϵ to reduce the perturbation size. DDN combines the effectiveness of boundary attacks with the simplicity and per-step speed of soft-constraint attacks; however, it is specific to the ℓ_2 norm and cannot be readily extended to other norms.

To overcome the aforementioned limitations, in this work we propose a novel, fast minimum-norm (FMN) attack (Sect. 2), which retains the main advantages of DDN while generalizing it to different ℓ_p norms ($p = 0, 1, 2, \infty$). We perform large-scale experiments on different datasets and models

¹Department of Electrical and Electronic Engineering, University of Cagliari, Italy ²Pluribus One ³University of Tübingen, Germany. Correspondence to: Maura Pintor <maura.pintor@unica.it>.

(Sect. 3), showing that FMN is able to significantly outperform current minimum-norm attacks in terms of convergence speed and computation time, while finding equal or better optima across almost all tested scenarios and ℓ_p norms. FMN thus combines all desirable traits a good adversarial attack should have, providing an important step towards improving adversarial robustness evaluations. We conclude the paper by discussing related work (Sect. 4) and future research directions (Sect. 5).

2. Minimum-Norm Adversarial Examples with Adaptive Projections

Problem formulation. Given an input sample $\mathbf{x} \in [0, 1]^d$, belonging to class $y \in \{1, \dots, c\}$, the goal of an untargeted attack is to find the minimum-norm perturbation δ^* such that the corresponding adversarial example $\mathbf{x}^* = \mathbf{x} + \delta^*$ is misclassified. This problem can be formulated as:

$$\delta^* \in \arg \min_{\delta} \quad \|\delta\|_p, \quad (1)$$

$$\text{s.t.} \quad L(\mathbf{x} + \delta, y, \theta) < 0, \quad (2)$$

$$\mathbf{x} + \delta \in [0, 1]^d, \quad (3)$$

where $\|\cdot\|_p$ indicates the ℓ_p -norm operator. The loss function L in the constraint in Eq. (2) is defined as:

$$L(\mathbf{x}, y, \theta) = f_y(\mathbf{x}, \theta) - \max_{j \neq y} f_j(\mathbf{x}, \theta), \quad (4)$$

where $f_j(\mathbf{x}, \theta)$ is the confidence given by the model f for classifying \mathbf{x} as class j , and θ is the set of its learned parameters. Assuming that the classifier assigns \mathbf{x} to the class exhibiting the highest confidence, i.e., $y^* = \arg \max_{j \in \{1, \dots, c\}} f_j(\mathbf{x}, \theta)$, the loss function $L(\mathbf{x}, y, \theta)$ takes on negative values only when \mathbf{x} is misclassified. Finally, the box constraint in Eq. (3) ensures that the perturbed sample $\mathbf{x} + \delta$ lies in the feasible input space.

The aforementioned problem typically involves a non-convex loss function L (w.r.t. its first argument), due to the non-convexity of the underlying decision function f . For this reason, it may admit different locally-optimal solutions. Note also that the solution is trivial (i.e., $\delta^* = \mathbf{0}$) when the input sample \mathbf{x} is already adversarial (i.e., $L(\mathbf{x}, y, \theta) < 0$).

Extension to the targeted case. The goal of a targeted attack is to have the input sample misclassified in a given target class y' . This can be accounted for by modifying the loss function in Eq. (4) as $L^t(\mathbf{x}, y', \theta) = \max_{j \neq y'} f_j(\mathbf{x}, \theta) - f_{y'}(\mathbf{x}, \theta) = -L(\mathbf{x}, y', \theta)$, i.e., changing its sign and using the target class label y' instead of the true class label y .

Solution algorithm. To solve the optimization in Eqs. (1)-(3), we reformulate it introducing an upper bound ϵ on $\|\delta\|_p$:

$$\min_{\epsilon, \delta} \quad \epsilon, \quad (5)$$

$$\text{s.t.} \quad \|\delta\|_p \leq \epsilon, \quad (6)$$

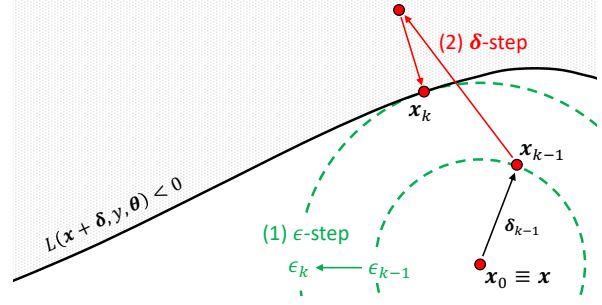


Figure 1. Conceptual representation of the FMN attack (Algorithm 1). The ϵ -step updates the constraint size ϵ to minimize its distance to the boundary. The δ -step updates the perturbation δ with a projected-gradient step to maximize misclassification confidence within the current ϵ -sized constraint.

and to the constraints in Eqs. (2)-(3). This allows us to derive an algorithm that works in two main steps, similarly to DDN (Rony et al., 2019), by updating the maximum perturbation size ϵ separately from the actual perturbation δ , as represented in Fig. 1. In particular, the constraint size ϵ is adapted to reduce the distance of the constraint to the boundary (ϵ -step), while the perturbation δ is updated using a projected-gradient step to minimize the loss function L within the given ϵ -sized constraint (δ -step). This essentially amounts to a projected gradient descent algorithm that iteratively adapts the constraint size ϵ to find the minimum-norm adversarial example. The complete algorithm is given as Algorithm 1, while a more detailed explanation of the two aforementioned steps is given below.

ϵ -step. This step updates the upper bound ϵ on the perturbation norm (lines 4-16 in Algorithm 1). The underlying idea is to increase ϵ if the current sample is not adversarial (i.e., $L(\mathbf{x}_{k-1}, y, \theta) \geq 0$), and to decrease it otherwise, while reducing the step size to dampen oscillations around the boundary and reach convergence.

ϵ -increase. In the former case, the increment of ϵ depends on whether an adversarial example has been previously found or not. If not, we estimate the distance to the boundary with a first-order linear approximation, and set $\epsilon_k = \|\delta_{k-1}\|_p + L(\mathbf{x}_{k-1}, y, \theta) / \|\nabla L(\mathbf{x}_{k-1}, y, \theta)\|_q$, being q the dual norm of p . This approximation allows the attack point to make faster progress towards the decision boundary. Conversely, if an adversarial sample has been previously found, but the current sample is not adversarial, it is likely that the current estimate of ϵ is only slightly smaller than the minimum-norm solution. We thus increase ϵ by a small fraction as $\epsilon_k = \epsilon_{k-1} (1 + \gamma_k)$, where γ_k is a decaying step size.

ϵ -decrease. If the current sample is adversarial, i.e., $L(\mathbf{x}_{k-1}, y, \theta) < 0$, we decrease ϵ as $\epsilon_k = \epsilon_{k-1} (1 - \gamma_k)$, to check whether the current solution can be improved. If the corresponding ϵ_k value is larger than the optimal $\|\delta^*\|_p$

Algorithm 1 Fast Minimum-norm (FMN) Attack

Input: \mathbf{x} , the input sample; t , a variable denoting whether the attack is targeted ($t = +1$) or untargeted ($t = -1$); y , the target (true) class label if the attack is targeted (untargeted); γ_0 and γ_K , the initial and final ϵ -step sizes; α_0 and α_K , the initial and final δ -step sizes; K , the total number of iterations.

Output: The minimum-norm adversarial example \mathbf{x}^* .

```

1:  $\mathbf{x}_0 \leftarrow \mathbf{x}$ ,  $\epsilon_0 = 0$ ,  $\delta_0 \leftarrow \mathbf{0}$ ,  $\delta^* \leftarrow \infty$ 
2: for  $k = 1, \dots, K$  do
3:    $\mathbf{g} \leftarrow t \cdot \nabla_{\delta} L(\mathbf{x}_{k-1} + \delta, y, \theta)$  // loss gradient
4:    $\gamma_k \leftarrow h(\gamma_0, \gamma_K, k, K)$  //  $\epsilon$ -step size decay (Eq. 7)
5:   if  $L(\mathbf{x}_{k-1}, y, \theta) \geq 0$  then
6:     if adversarial has not been found yet then
7:        $\epsilon_k = \|\delta_{k-1}\|_p + L(\mathbf{x}_{k-1}, y, \theta) / \|\mathbf{g}\|_q$ 
8:     else
9:        $\epsilon_k = \epsilon_{k-1}(1 + \gamma_k)$ 
10:    end if
11:  else
12:    if  $\|\delta_{k-1}\|_p \leq \|\delta^*\|_p$  then
13:       $\delta^* \leftarrow \delta_{k-1}$  // update best min-norm solution
14:    end if
15:     $\epsilon_k = \min(\epsilon_{k-1}(1 - \gamma_k), \|\delta^*\|_p)$ 
16:  end if
17:   $\alpha_k \leftarrow h(\alpha_0, \alpha_K, k, K)$  //  $\delta$ -step size decay (Eq. 7)
18:   $\delta_k \leftarrow \delta_{k-1} + \alpha_k \cdot \mathbf{g} / \|\mathbf{g}\|_2$ 
19:   $\delta_k \leftarrow \Pi_{\epsilon}(\mathbf{x}_0 + \delta_k) - \mathbf{x}_0$ 
20:   $\delta_k \leftarrow \text{clip}(\mathbf{x}_0 + \delta_k) - \mathbf{x}_0$ 
21:   $\mathbf{x}_k \leftarrow \mathbf{x}_0 + \delta_k$ 
22: end for
23: return  $\mathbf{x}^* \leftarrow \mathbf{x}_0 + \delta^*$ 

```

found so far, we retain the best value and set $\epsilon_k = \|\delta^*\|_p$.

These multiplicative updates of ϵ exhibit an oscillating behavior around the decision boundary, due to the conflicting requirements of minimizing the perturbation size and finding an adversarial point. To ensure convergence, as anticipated before, the step size γ_k is decayed with cosine annealing:

$$\gamma_k = h(\gamma_0, \gamma_K, k, K) = \gamma_K + \frac{1}{2}(\gamma_0 - \gamma_K) \left(1 + \cos\left(\frac{k\pi}{K}\right)\right), \quad (7)$$

where k is the current step, K is the total number of steps, and γ_0 and γ_K are the initial and final step sizes.

δ -step. This step updates δ (lines 17-21 in Algorithm 1). The goal is to find the adversarial example that is misclassified with maximum confidence (i.e., for which L is minimized) within the current ϵ -sized constraint (Eq. 6) and bounds (Eq. 3). This amounts to performing a projected-gradient step along the negative gradient of L . We consider a normalized steepest descent with decaying step size α to overcome potential issues related to noisy gradients while ensuring convergence (line 18). The step size α is decayed

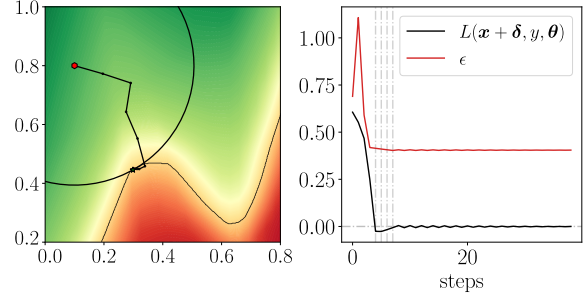


Figure 2. Example of execution of our attack on a bi-dimensional problem (left), along with the corresponding values of the loss function L and the constraint size ϵ across iterations (right). Our algorithm works by first pushing the initial point (red dot) towards the adversarial region (in red), and then perturbing it around the decision boundary to improve the current solution towards a local optimum. The vertical lines in the rightmost plot highlight the steps in which a better solution (smaller $\|\delta^*\|$ and $L < 0$) is found.

using cosine annealing (Eq. 7). Once δ is updated, we project it onto the given ϵ -sized ℓ_p -norm constraint via a projection operator Π_{ϵ} (line 19), to fulfill the constraint in Eq. (6). The projection is trivial for $p = \infty$ and $p = 2$. For $p = 1$, we use the efficient algorithm by Duchi et al. (2008). For $p = 0$, we retain only the first ϵ components of δ exhibiting the largest absolute value. We finally clip the components of δ that violate the bounds in Eq. (3) (line 20).

Execution example. In Fig. 2, we report an example of execution of our algorithm on a bi-dimensional problem. The initial sample is updated to follow the negative gradient of L towards the decision boundary. When an adversarial point is found, the algorithm reduces ϵ in search of a better solution. The point is thus projected back onto the non-adversarial region, and ϵ increased (though by a smaller, decaying amount). This oscillating behavior allows the point to walk on the boundary towards a local optimum, i.e., an adversarial point lying on the boundary, where the gradient of the loss function and that of the norm constraint have opposite direction. Our algorithm tends to quickly converge towards a good local optimum, provided that the step size is reduced to a sufficiently-small value and that a sufficiently-large number of iterations are performed. This is also confirmed by the extensive experiments in Sect. 3.

Adversarial initialization. Our attack can be initialized either from the given sample \mathbf{x} , or from a point \mathbf{x}_{init} belonging to a different class (if the attack is untargeted) or to the target class (if the attack is targeted). When initializing the attack from \mathbf{x}_{init} , we perform a 10-step binary search between \mathbf{x} and \mathbf{x}_{init} , to find an adversarial point which is closer to the decision boundary. In particular, we aim to find the minimum ϵ such that $L(\mathbf{x} + \Pi_{\epsilon}(\mathbf{x}_{\text{init}} - \mathbf{x}), y, \theta) < 0$ (or $L^t < 0$ for targeted attacks). Then we run our attack

starting from the corresponding values of x_k , ϵ_k , δ_k and δ^* .

Differences with DDN. FMN applies substantial changes to both the algorithm and the formulation of DDN. The main difference is that (i) DDN always rescales the perturbation to have size ϵ . This operation is problematic when using other norms, especially sparse ones, as it makes it more difficult for the attack to properly explore the neighboring space and find a suitable descent direction. Another difference with DDN is that (ii) FMN does not use the cross-entropy loss but rather the logit difference as the loss function L . Moreover, (iii) FMN does not need an initial value for ϵ , as ϵ is dynamically estimated. We also apply (iv) a decay on γ to improve convergence around better minimum-norm solutions, by more effectively dampening oscillations around the boundary. Finally, we include the possibility of (v) initializing the attack from an adversarial point, which can greatly increase the convergence speed of the algorithm.

3. Experiments

We report here an extensive experimental analysis involving several state-of-the-art defenses and minimum-norm attacks, covering ℓ_0 , ℓ_1 , ℓ_2 and ℓ_∞ norms. The goal is to empirically benchmark our attack and assess its effectiveness and efficiency as a tool for adversarial robustness evaluation.

3.1. Experimental Setup

Datasets. We consider two commonly-used datasets for benchmarking adversarial robustness of deep neural networks, i.e., the MNIST handwritten digits and CIFAR10. Following the experimental setup in Brendel et al. (2019), we use a subset of 1000 test samples to evaluate the performances of the considered attacks and defenses.

Models. We use a diverse selection of models to thoroughly evaluate attacks under different conditions. We select three different models per dataset, denoted with M1, M2, M3 for MNIST, and C1, C2, C3 for CIFAR10, as detailed below.

For MNIST, we consider the following models: *M1*, the 9-layer network used as the undefended baseline model by Papernot et al. (2016); Carlini & Wagner (2017); *M2*, the robust model by Madry et al. (2017), trained on ℓ_∞ attacks (robustness claim: 89.6% accuracy with $\|\delta\|_\infty \leq 0.3$, current best evaluation: 88.0%); and *M3*, the robust model by Rony et al. (2019), trained on ℓ_2 attacks (robustness claim: 87.6% accuracy with $\|\delta\|_2 \leq 1.5$).

For CIFAR10, we consider three state-of-the-art robust models from RobustBench (Croce et al., 2020): *C1*, the robust model by Madry et al. (2017), trained on ℓ_∞ attacks (robustness claim: 44.7% accuracy with $\|\delta\|_\infty \leq 8/255$, current best evaluation: 44.0%); *C2*, the defended model by Carmon et al. (2019) (top-5 in RobustBench), trained on ℓ_∞

attacks and additional unsupervised data (robustness claim: 62.5% accuracy with $\|\delta\|_\infty \leq 8/255$, current best evaluation: 59.5%); and *C3*, the robust model by Rony et al. (2019), trained on ℓ_2 attacks (robustness claim: 67.9% accuracy with $\|\delta\|_2 \leq 0.5$, current best evaluation: 66.4%).

Attacks. We compare our algorithm against different state-of-the-art attacks for finding minimum-norm adversarial perturbations across different norms: the Carlini & Wagner (CW) attack (Carlini & Wagner, 2017), the Decoupling Direction and Norm (DDN) attack (Rony et al., 2019), the Brendel & Bethge (BB) attack (Brendel et al., 2019), and the Fast Adaptive Boundary (FAB) attack (Croce & Hein, 2020b). We use the implementation of FAB from Ding et al. (2019), while for all the remaining attacks we use the implementation available in Foolbox (Raubert et al., 2017; 2020). All these attacks are defined on the ℓ_2 norm. BB and FAB are also defined on the ℓ_1 and ℓ_∞ norms, and only BB is defined on the ℓ_0 norm. We consider both untargeted and targeted attack scenarios, as defined in Sect. 2, except for FAB, which is only evaluated in the untargeted case.¹

Hyperparameters. To ensure a fair comparison, we perform an extensive hyperparameter search for each of the considered attacks. The optimal hyperparameters are selected *separately for each input sample*, by running each attack from 10 to 16 times per sample, with a different hyperparameter configuration or random initialization point each time. We select the hyperparameters to be optimized for each attack as done by Brendel et al. (2019), and as recommended by the corresponding authors (Carlini & Wagner, 2017; Croce & Hein, 2020b; Rony et al., 2019). The hyperparameter configurations considered for each attack are detailed below. For attacks that are robust to hyperparameter changes, like BB and FAB, we follow the recommendation of using a larger number of random starts rather than increasing the number of hyperparameter configurations to be tested. In addition, as BB requires being initialized from an adversarial starting point, we initialize it by randomly selecting a sample either from a different class (in the untargeted case) or from the target class (in the targeted case). Finally, as each attack performs operations with different levels of complexity within each iteration, possibly querying the model multiple times, we set the number of steps for each attack such that at least 1,000 queries are performed. This ensures a fairer comparison also in terms of the computational time and resources required to execute each attack.

CW. This attack minimizes the soft-constraint version of our problem, i.e., $\min_{\delta} \|\delta\|_p + c \cdot \min(L(x + \delta, y, \theta), -\kappa)$.

¹The reason is that FAB implements a substantially different attack in the targeted case. The targeted version of FAB aims to find a closer untargeted misclassification by running the attack a number of times, each time targeting a different candidate class, and then selecting the best solution (Croce & Hein, 2020b;a).

The hyperparameters κ and c are used to tune the trade-off between perturbation size and misclassification confidence. To find minimum-norm perturbations, CW requires setting $\kappa = 0$, while the constant c is tuned via binary search (re-running the attack at each iteration). We set the number of binary-search steps to 9, and the maximum number of iterations to 250, to ensure that at least 1,000 queries are performed. We also consider different initial values for c and the step size η , i.e., $c, \eta \in \{10^{-3}, 10^{-2}, 10^{-1}, 1\}$.

DDN. This attack, similarly to ours, maximizes the misclassification confidence within an ϵ -sized constraint, while adjusting ϵ to minimize the perturbation size. We consider initial values of $\epsilon_0 \in \{0.03, 0.1, 0.3, 1, 3\}$, and run the attack with a different number of iterations $K \in \{200, 1000\}$, as this affects the size of each update on δ .

BB. This attack starts from a randomly-drawn adversarial point, performs a 10-step binary search to find a point which is closer to the decision boundary, and then updates the point to minimize its perturbation size by following the decision boundary. In each iteration, BB computes the optimal update within a given trust region of radius ρ . We consider different values for $\rho \in \{10^{-3}, 10^{-2}, 10^{-1}, 1\}$, while we fix the number of steps to 1000. We run the attack 3 times by considering different initialization points, and eventually retain the best solution.

FAB. This attack iteratively optimizes the attack point by linearly approximating its distance to the decision boundary. It uses an adaptive step size bounded by α_{\max} and an extrapolation step η to facilitate finding adversarial points. As suggested by Croce & Hein (2020b), we tune $\alpha_{\max} \in \{0.1, 0.05\}$ and $\eta \in \{1.05, 1, 3\}$. We consider 3 different random initialization points, and run the attack for 500 steps each time, eventually selecting the best solution.

FMN. We run our attack for $K = 1000$ steps. For ℓ_0, ℓ_1 , and ℓ_2 , we use $\alpha_0 \in \{1, 5, 10\}$ and $\gamma_0 \in \{0.05, 0.3\}$. For ℓ_∞ , we use the same values for γ_0 but $\alpha_0 \in \{10^1, 10^2, 10^3\}$, as the normalized ℓ_2 step yields a much smaller update in the ℓ_∞ norm. We set $\gamma_K = 10^{-4}$, $\alpha_K = 10^{-5}$. For each hyperparameter setting we run the attack twice, starting from (i) the input sample and (ii) an adversarial point.

Evaluation criteria. We evaluate the attacks according to four different criteria: (i) *perturbation size*, measured as the median of $\|\delta^*\|_p$ on the testing points, using the best hyperparameters for each point, and within a given budget of Q queries to the model; (ii) *execution time*, measured as the average time spent per query (in milliseconds); (iii) *convergence speed*, measured as the average number of queries required to converge to a good-enough solution (within 10% of the best value found at $Q = 1000$); and (iv) *robustness to hyperparameter selection*, measured as the average increase of the optimal perturbation size when the

hyperparameters are still optimized but kept equal for all testing points (i.e., optimized at the dataset-level rather than at the sample-level).

3.2. Experimental Results

Query-distortion curves. To evaluate each attack in terms of perturbation size under the same query budget Q , we use the so-called query-distortion curves introduced by Brendel et al. (2019). These curves report, for each attack, the median value of δ^* as a function of the number of queries Q . For each given Q value, the optimal δ^* for each point is selected among the different attack executions (i.e., using different hyperparameters and/or initialization points, as described in Sect. 3.1). In Fig. 3, we report the query-distortion curves for the MNIST and CIFAR10 challenge models (i.e., M2 and C1) in the untargeted scenario. The remaining query-distortion curves exhibit a similar behavior and can be found in the supplementary material. It is worth noting that our attack attains comparable results in terms of perturbation size across all norms, while significantly outperforming FAB and BB in the ℓ_1 case. It typically requires also less iterations than the other attacks to converge. While the query-distortion curves show the complete behavior of each attack as Q increases, a more compact and thorough summary of our evaluation is reported below, according to the four evaluation criteria described in Sect. 3.1.

Perturbation size. Table 1 reports the median value of $\|\delta^*\|$ at $Q = 1000$ queries (i.e., the last value from the query-distortion curve), for all models, attacks and norms. The reported values confirm that our attack finds smaller or comparable perturbations to that found by the competing attacks, both in the untargeted and targeted case, and that the biggest margin is achieved by our ℓ_1 attack. Our attack is slightly worse than BB in the ℓ_∞ and ℓ_0 case on the MNIST challenge model (M2), even though being comparable to FAB in the former case. The reason is that optimizing the attack samples against this model is particularly challenging, due to the presence of noisy gradients and flat regions around the clean input samples, which makes it difficult for FMN and FAB to quickly find a suitable descent direction.

Execution time. The average runtime per query for each attack-model pair, measured on a workstation with an NVIDIA GeForce RTX 2080 Ti GPU with 12GB of RAM, can be found in Table 2. The results show that our attack is up to 2-3 times faster, with the exception of DDN in the ℓ_2 case. This is however compensated by the fact that FMN finds better solutions. The advantage is that our attack avoids costly inner projections as in BB and FAB. FMN is slightly less time-efficient than DDN and CW, as it simultaneously updates the adversarial point and the norm constraint. In particular, the update on the constraint may initially require computing the norm of the gradient g (line 7

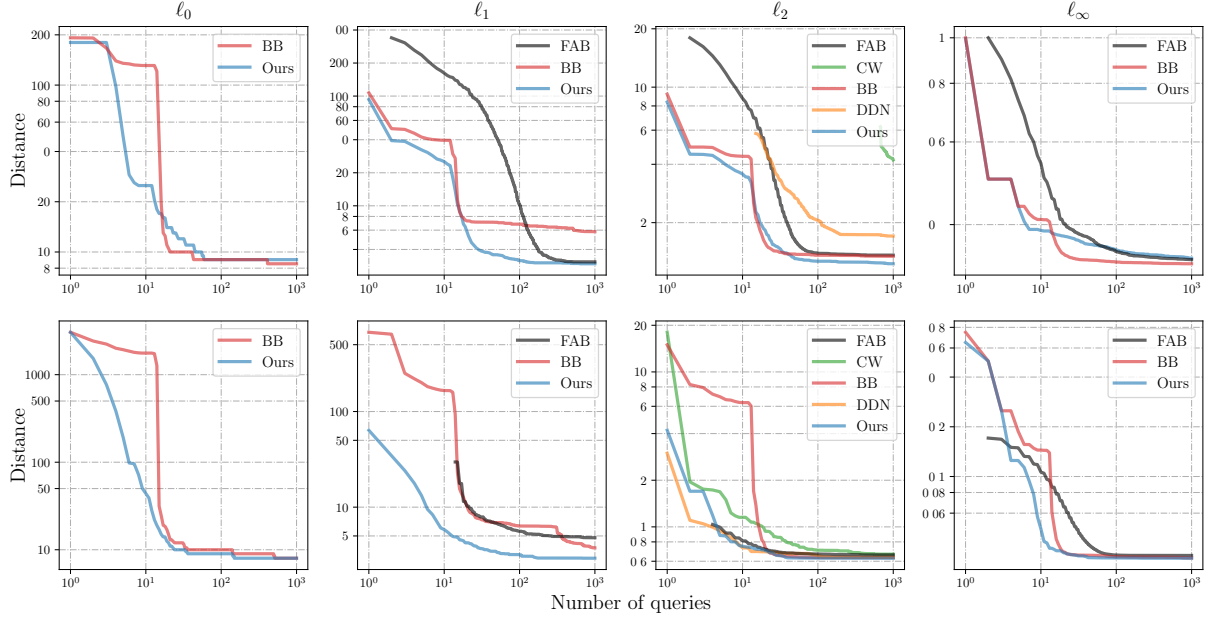


Figure 3. Query-distortion curves for MNIST (M2) and CIFAR10 (C1) challenge models in the untargeted scenario.

Table 1. Median $\|\delta^*\|_p$ value at $Q = 1000$ queries for targeted and untargeted attacks, with hyperparameters optimized for each sample.

		MNIST						CIFAR10					
		Untargeted			Targeted			Untargeted			Targeted		
Model		M1	M2	M3	M1	M2	M3	C1	C2	C3	C1	C2	C3
ℓ_0	BB	7	8	15	14	27	24	8	12	13	19	32	25
	Ours	7	9	15	14	32	24	8	11	14	18	31	26
ℓ_1	FAB	6.596	3.083	14.232	-	-	-	4.787	5.175	8.786	-	-	-
	BB	6.255	5.813	13.158	12.417	10.377	20.410	3.748	4.294	8.620	8.036	10.931	15.713
	Ours	5.551	2.963	12.041	12.174	7.060	18.792	2.923	3.409	8.156	6.948	9.270	15.576
ℓ_2	FAB	1.449	1.360	2.624	-	-	-	0.659	0.720	0.936	-	-	-
	CW	1.490	4.216	2.782	2.326	6.968	3.541	0.667	0.741	0.911	1.076	1.272	1.383
	BB	1.431	1.342	2.613	2.275	2.039	3.231	0.634	0.704	0.909	1.067	1.265	1.378
	DDN	1.463	1.705	2.564	2.286	2.199	3.275	0.637	0.727	0.910	1.092	1.285	1.390
	Ours	1.406	1.227	2.503	2.279	1.909	3.189	0.628	0.700	0.909	1.022	1.204	1.375
ℓ_∞	FAB	0.138	0.337	0.233	-	-	-	0.033	0.043	0.025	-	-	-
	BB	0.138	0.330	0.227	0.202	0.355	0.271	0.032	0.041	0.024	0.055	0.064	0.037
	Ours	0.134	0.339	0.223	0.201	0.389	0.271	0.032	0.040	0.024	0.055	0.063	0.037

in Algorithm 1), which increases the runtime of our attack. FAB computes a similar step, but for all the output classes, which hinders its scalability to problems with many classes.

Convergence speed. To get an estimate of the convergence speed, we measure the number of queries required by each attack to reach a perturbation size that is within 10% of the value found at $Q = 1000$ queries (the lower the better). Results are shown in Table 3. Our attack converges on par with or faster than all other attacks for almost all models, often requiring only half or a fifth as many queries as the state of the art. Exceptions are MNIST and CIFAR10 challenge

models (M2 and C1) for ℓ_2 and ℓ_∞ , where BB and DDN occasionally converge faster. FMN rarely needs more than 100 steps, and tends to reach the minimal perturbation after only 10-30 queries on many datasets, models and norms.

Robustness to hyperparameter selection. Selecting the optimal hyperparameters for each point is computationally demanding and rarely done in practice. It is thus of interest to evaluate how sensitive an attack is to a suboptimal selection of its hyperparameters. To this end, we optimize the hyperparameters at the dataset-level (i.e., using the same configuration for all testing points) and measure the differ-

Table 2. Average execution time (milliseconds / query) for each attack-model pair.

		MNIST						CIFAR10					
Model		Untargeted			Targeted			Untargeted			Targeted		
		M1	M2	M3	M1	M2	M3	C1	C2	C3	C1	C2	C3
ℓ_0	BB	10.76	11.85	10.19	60.88	62.17	62.31	46.51	50.31	50.43	99.71	105.28	103.53
	Ours	5.15	4.87	5.87	5.14	4.75	5.85	26.26	30.54	30.89	26.13	30.26	30.81
ℓ_1	FAB	9.38	8.88	12.61	-	-	-	84.04	108.91	108.64	-	-	-
	BB	6.73	7.03	7.31	43.25	43.54	43.69	32.56	37.40	37.59	68.99	73.33	74.03
	Ours	5.43	5.14	6.10	5.44	5.10	6.09	27.34	31.17	31.18	26.00	30.98	31.03
ℓ_2	FAB	10.22	10.13	13.45	-	-	-	84.27	109.43	108.87	-	-	-
	CW	4.22	4.09	5.17	4.23	4.14	5.15	25.90	31.32	31.31	25.78	31.32	31.30
	BB	4.44	4.15	5.03	26.20	26.76	27.24	26.64	31.82	31.90	48.74	54.35	54.07
	DDN	3.42	3.33	4.30	3.42	3.35	4.32	24.14	29.62	29.48	23.61	29.61	29.52
	Ours	4.46	4.42	5.48	4.50	4.44	5.47	24.88	30.22	30.08	25.39	30.21	30.04
ℓ_∞	FAB	10.85	10.61	14.05	-	-	-	84.62	109.83	109.57	-	-	-
	BB	14.26	16.36	13.51	38.61	38.87	36.39	61.34	62.36	62.63	83.70	87.64	88.90
	Ours	4.25	4.33	5.30	4.33	4.23	5.31	24.84	30.15	30.01	24.78	30.19	30.03

Table 3. Number of queries required by each attack to reach a perturbation size that is within 10% of the value obtained at $Q = 1000$.

		MNIST						CIFAR10					
Model		Untargeted			Targeted			Untargeted			Targeted		
		M1	M2	M3	M1	M2	M3	C1	C2	C3	C1	C2	C3
ℓ_0	BB	22	43	68	30	443	71	497	372	58	384	500	85
	Ours	18	56	38	31	43	46	142	142	37	159	135	81
ℓ_1	FAB	44	242	152	-	-	-	124	220	72	-	-	-
	BB	24	314	83	45	614	233	674	570	34	526	464	206
	Ours	22	87	34	24	118	37	73	43	22	111	52	47
ℓ_2	FAB	14	60	40	-	-	-	18	28	14	-	-	-
	CW	110	799	335	100	913	469	67	39	33	56	144	42
	BB	20	24	20	21	61	20	22	23	22	26	27	29
	DDN	12	136	15	12	149	26	13	20	4	18	19	18
	Ours	8	45	16	11	47	16	22	16	9	28	31	15
ℓ_∞	FAB	36	50	44	-	-	-	50	50	54	-	-	-
	BB	19	17	20	24	17	22	20	24	21	27	33	29
	Ours	17	28	22	33	9	26	19	27	14	30	36	37

ence to the case in which they are optimized at the sample-level. Results are reported in Table 4. The accuracy drop of FMN and DDN is negligible, while other attacks like BB suffer when using the same hyperparameters for all samples.

Robust accuracy. Despite our attack being not tailored to target specific defenses, and our evaluation restricted to a subset of the testing samples, it is worth remarking that the robust accuracies of the models against our attack are aligned with that reported in current evaluations, with the notable exception of C3, where our attack can decrease robust accuracy from 67.9% to 65.5%.

4. Related Work

Gradient-based attacks on machine learning have a long history (Biggio et al., 2013; Biggio & Roli, 2018). They can be categorized in two main classes: minimum-norm and maximum-confidence attacks. Maximum-confidence attacks optimize the adversarial loss (e.g., the difference between the logits of the true class and the best non-true class) to find an adversarial point misclassified with maximum confidence within a given, bounded perturbation size. While attacks in this category like FGSM (Goodfellow et al., 2015), PGD (Kurakin et al., 2016; Madry et al., 2017) and momentum-based extensions of PGD (Uesato et al., 2018; Dong et al., 2018) are popular, they only partially evaluate the adversarial robustness of a model.

Table 4. Robustness to hyperparameters, measured as the difference between the perturbation size obtained when the hyperparameters are optimized at the dataset-level and that obtained when the hyperparameters are optimized at the sample-level (the lower the better).

		MNIST						CIFAR10					
Model		Untargeted			Targeted			Untargeted			Targeted		
		M1	M2	M3	M1	M2	M3	C1	C2	C3	C1	C2	C3
ℓ_0	BB	3	16	7	1	21	7	4	7	3	6	11	3
	Ours	0	7	2	1	9	2	2	2	1	5	4	3
ℓ_1	FAB	0.497	4.274	1.839	-	-	-	0.617	1.103	1.285	-	-	-
	BB	3.747	10.653	7.215	1.801	7.047	5.324	1.120	1.218	3.099	1.906	0.911	3.181
	Ours	0.149	1.675	0.649	0.178	1.740	0.867	0.571	0.390	0.324	0.569	0.407	0.756
ℓ_2	FAB	0.087	0.329	0.128	-	-	-	0.035	0.054	0.025	-	-	-
	CW	0.046	-	0.283	0.031	-	1.073	0.034	0.002	0.003	0.010	0.031	0.012
	BB	0.494	0.568	0.697	0.099	0.461	0.252	0.194	0.144	0.117	0.154	0.122	0.084
	DDN	0.018	0.316	0.068	0.013	0.388	0.032	0.011	0.017	0.000	0.017	0.026	0.002
	Ours	0.008	0.205	0.023	0.002	0.155	0.011	0.001	0.001	0.000	0.032	0.028	0.001
ℓ_∞	FAB	0.010	0.012	0.012	-	-	-	0.005	0.005	0.002	-	-	-
	BB	0.036	0.008	0.027	0.006	0.005	0.006	0.007	0.005	0.003	0.003	0.004	0.000
	Ours	0.000	0.012	0.001	0.001	0.033	0.002	0.000	0.001	0.000	0.000	0.001	0.000

Minimum-norm attacks aim to minimize the norm of the perturbation subject to being adversarial. Attacks from this class give a more complete picture of the model robustness and allow us to compute the accuracy of the model under attacks with any post-hoc defined maximum perturbation size. L-BFGS (Szegedy et al., 2014) solves this problem with a quasi-Newton optimizer while CW (Carlini & Wagner, 2017) and EAD (Chen et al., 2017) use first-order gradient-based optimizers to minimize a weighted loss between perturbation size and misclassification confidence. To find the smallest adversarial perturbation, both CW and EAD need to tune the relative weighting which makes them query-inefficient. DeepFool (Moosavi-Dezfooli et al., 2016) and SparseFool (Modas et al., 2019) compute gradients with respect to all classes in each step to estimate a linear approximation of the model from which the optimal adversarial perturbation can be computed. These two attacks are fast but do not converge to competitive solutions. BB (Brendel et al., 2019) and FAB (Croce & Hein, 2020b) use complex projections and approximations to stay close to the decision boundary (using the gradient to estimate the local geometry of the boundary) while minimizing the norm. This way of formulating the minimum-norm optimization problem bypasses the tuning of a weighting term, but in the case of BB also requires an adversarial starting point to begin with. The DDN attack (Rony et al., 2019) maximizes the adversarial criterion within a given norm constraint, and iteratively reduces the norm to find the smallest possible adversarial perturbation. However, it is constrained to ℓ_2 and does not perform well on other ℓ_p norms.

The proposed FMN attack belongs to the category of minimum-norm attacks, and builds on BB, FAB and DDN to retain their main advantages. First, FMN is not specific to

a given norm, and converges in much fewer steps than soft-constraint attacks like CW, as it does not need to optimize the trade-off between perturbation size and misclassification confidence. FMN needs significantly less computational time per step than the other attacks, it is very accurate and easy to use, and it does not necessarily require being initialized from an adversarial starting point.

5. Conclusions and Future Work

This work introduces a novel minimum-norm attack that combines all desirable traits to help improve current adversarial evaluations: (i) finding smaller or comparable minimum-norm perturbations across a range of models and datasets; being extremely fast, by (ii) reducing runtime up to 3 times per query with respect to competing attacks and (iii) converging within less iterations; and (iv) being insensitive to hyperparameter choices. FMN also works with different ℓ_p norms ($p = 0, 1, 2, \infty$) and it does not necessarily require being initialized from an adversarial starting point.

We also believe that FMN may facilitate minimum-norm adaptive evaluations. Adaptive evaluations, where the attack is modified to be maximally effective against a new defense, are the key element towards properly evaluating adversarial robustness (Carlini et al., 2019; Tramer et al., 2020). Gradient-projected (PGD) attacks are popular in part for the ease by which they can be adapted to new defenses. Since FMN combines PGD with a dynamic minimization of the perturbation size, we argue that our attack can also be easily adapted to new defenses. Most likely, FMN will also benefit from improvements that have been suggested for PGD, including momentum, cyclical step sizes or restarts. We leave such improvements to future work.

We firmly believe that FMN will establish itself as a useful tool in the arsenal of robustness evaluation. It rivals or surpasses other attacks in speed, reliability, efficacy and versatility. By facilitating more reliable robustness evaluations, we hope that the field of adversarial robustness will be able to more quickly identify the most promising avenues towards more robust machine learning algorithms.

Acknowledgements

F. Roli, B. Biggio and M. Pintor would like to acknowledge support from the PRIN 2017 project RexLearn (grant no. 2017TWNMH2), funded by the Italian Ministry of Education, University and Research; and from BMK, BMDW, and the Province of Upper Austria in the frame of the COMET Programme managed by FFG in the COMET Module S3AI. W. Brendel acknowledges support from the German Federal Ministry of Education and Research (BMBF) through the Competence Center for Machine Learning (TUE.AI, FKZ 01IS18039A), from the German Science Foundation (DFG) under grant no. BR 6382/1-1 (Emmy Noether Program) as well as support by Open Philanthropy and the Good Ventures Foundation.

References

- Athalye, A., Carlini, N., and Wagner, D. A. Obfuscated gradients give a false sense of security: Circumventing defenses to adversarial examples. In *ICML*, volume 80 of *JMLR Workshop and Conference Proceedings*, pp. 274–283. JMLR.org, 2018.
- Biggio, B. and Roli, F. Wild patterns: Ten years after the rise of adversarial machine learning. *Pattern Recognition*, 84:317–331, 2018.
- Biggio, B., Corona, I., Maiorca, D., Nelson, B., Šrndić, N., Laskov, P., Giacinto, G., and Roli, F. Evasion attacks against machine learning at test time. In Blockeel, H., Kersting, K., Nijssen, S., and Železný, F. (eds.), *Machine Learning and Knowledge Discovery in Databases (ECML PKDD), Part III*, volume 8190 of *LNCS*, pp. 387–402. Springer Berlin Heidelberg, 2013.
- Brendel, W., Rauber, J., Kümmeler, M., Ustyuzhaninov, I., and Bethge, M. Accurate, reliable and fast robustness evaluation. In *Advances in Neural Information Processing Systems*, pp. 12861–12871, 2019.
- Carlini, N. and Wagner, D. Towards evaluating the robustness of neural networks. In *2017 IEEE Symposium on Security and Privacy (SP)*, pp. 39–57. IEEE, 2017.
- Carlini, N., Athalye, A., Papernot, N., Brendel, W., Rauber, J., Tsipras, D., Goodfellow, I., Madry, A., and Kurakin, A. On evaluating adversarial robustness. *arXiv preprint arXiv:1902.06705*, 2019.
- Carmon, Y., Raghuathan, A., Schmidt, L., Duchi, J. C., and Liang, P. S. Unlabeled data improves adversarial robustness. In *Advances in Neural Information Processing Systems*, pp. 11192–11203, 2019.
- Chen, P.-Y., Sharma, Y., Zhang, H., Yi, J., and Hsieh, C.-J. Ead: elastic-net attacks to deep neural networks via adversarial examples. *arXiv preprint arXiv:1709.04114*, 2017.
- Croce, F. and Hein, M. Reliable evaluation of adversarial robustness with an ensemble of diverse parameter-free attacks. In *ICML*, 2020a.
- Croce, F. and Hein, M. Minimally distorted adversarial examples with a fast adaptive boundary attack. In *International Conference on Machine Learning*, pp. 2196–2205. PMLR, 2020b.
- Croce, F., Andriushchenko, M., Sehwag, V., Flammarion, N., Chiang, M., Mittal, P., and Hein, M. Robustbench: a standardized adversarial robustness benchmark. *arXiv preprint arXiv:2010.09670*, 2020.
- Ding, G. W., Wang, L., and Jin, X. AdverTorch v0.1: An adversarial robustness toolbox based on pytorch. *arXiv preprint arXiv:1902.07623*, 2019.
- Dong, Y., Liao, F., Pang, T., Su, H., Zhu, J., Hu, X., and Li, J. Boosting adversarial attacks with momentum. In *Proceedings of the IEEE Conference on Computer Vision and Pattern Recognition*, 2018.
- Duchi, J., Shalev-Shwartz, S., Singer, Y., and Chandra, T. Efficient projections onto the l_1 -ball for learning in high dimensions. In *Proceedings of the 25th international conference on Machine learning*, pp. 272–279, 2008.
- Goodfellow, I., Shlens, J., and Szegedy, C. Explaining and harnessing adversarial examples. In *International Conference on Learning Representations*, 2015. URL <http://arxiv.org/abs/1412.6572>.
- Kurakin, A., Goodfellow, I., and Bengio, S. Adversarial examples in the physical world. *arXiv preprint arXiv:1607.02533*, 2016.
- Madry, A., Makelov, A., Schmidt, L., Tsipras, D., and Vladu, A. Towards deep learning models resistant to adversarial attacks. *arXiv preprint arXiv:1706.06083*, 2017.
- Modas, A., Moosavi-Dezfooli, S.-M., and Frossard, P. Sparsefool: a few pixels make a big difference. In *The IEEE Conference on Computer Vision and Pattern Recognition (CVPR)*, 2019.

- Moosavi-Dezfooli, S.-M., Fawzi, A., and Frossard, P. Deep-fool: A simple and accurate method to fool deep neural networks. In *The IEEE Conference on Computer Vision and Pattern Recognition (CVPR)*, June 2016.
- Papernot, N., McDaniel, P., Wu, X., Jha, S., and Swami, A. Distillation as a defense to adversarial perturbations against deep neural networks. In *2016 IEEE symposium on security and privacy (SP)*, pp. 582–597. IEEE, 2016.
- Rauber, J., Brendel, W., and Bethge, M. Foolbox: A python toolbox to benchmark the robustness of machine learning models. In *Reliable Machine Learning in the Wild Workshop, 34th International Conference on Machine Learning*, 2017. URL <http://arxiv.org/abs/1707.04131>.
- Rauber, J., Zimmermann, R., Bethge, M., and Brendel, W. Foolbox native: Fast adversarial attacks to benchmark the robustness of machine learning models in pytorch, tensorflow, and jax. *Journal of Open Source Software*, 5(53):2607, 2020. doi: 10.21105/joss.02607. URL <https://doi.org/10.21105/joss.02607>.
- Rony, J., Hafemann, L. G., Oliveira, L. S., Ayed, I. B., Sabourin, R., and Granger, E. Decoupling direction and norm for efficient gradient-based l2 adversarial attacks and defenses. In *Proceedings of the IEEE Conference on Computer Vision and Pattern Recognition*, pp. 4322–4330, 2019.
- Szegedy, C., Zaremba, W., Sutskever, I., Bruna, J., Erhan, D., Goodfellow, I., and Fergus, R. Intriguing properties of neural networks. In *International Conference on Learning Representations*, 2014. URL <http://arxiv.org/abs/1312.6199>.
- Tramer, F., Carlini, N., Brendel, W., and Madry, A. On adaptive attacks to adversarial example defenses. In *Advances in Neural Information Processing Systems*, 2020.
- Uesato, J., O’Donoghue, B., Oord, A. v. d., and Kohli, P. Adversarial risk and the dangers of evaluating against weak attacks. *arXiv preprint arXiv:1802.05666*, 2018.

Appendix

In this section we first show adversarial examples obtained by different ℓ_p attacks on MNIST and CIFAR10 data for visual comparison. These examples highlight the different behavior exhibited by each attack. We then report the query-distortion curves for all datasets, models and attacks used in this paper, showing that our attack outperforms current attacks on the ℓ_1 norm and rivals their performance on other norms, while typically converging with much fewer queries.

A1. Adversarial Examples

In Figs. 1-8, we report adversarial examples generated by all attacks against model M2 and C2, respectively, on MNIST and CIFAR10 datasets, in the untargted scenario.

The clean samples and the original label are displayed in the first row of each figure. In the remaining rows we show the perturbed sample along with the predicted class and the corresponding norm of perturbation $\|\delta^*\|_p$. It is worth noting that the output class for different untargted attacks is not always the same, which might sometimes explain differences in the perturbation sizes. An example is given in Fig. 6, where the sample in the fourth column, labeled as “ship”, is perturbed by most of the attacks towards the class “airplane”, while in our case it outputs the class “dog” with a much smaller distance.

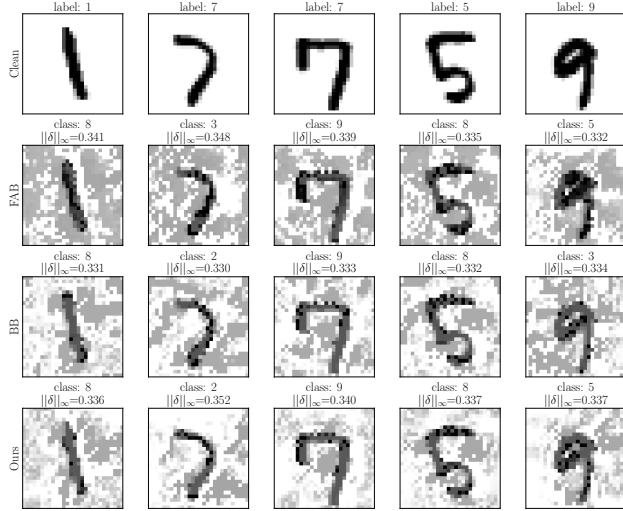


Figure 1. Untargeted ℓ_∞ attacks against M2 (Madry et al., 2017).

A2. Query-distortion Curves

In Sect. 3.2 we introduced the query-distortion curves as an efficiency evaluation metric for the attacks. We report here the complete results for all models, in targeted and untargted scenarios.

On the MNIST dataset, our attacks generally reach smaller



Figure 2. Untargeted ℓ_2 attacks against M2 (Madry et al., 2017).

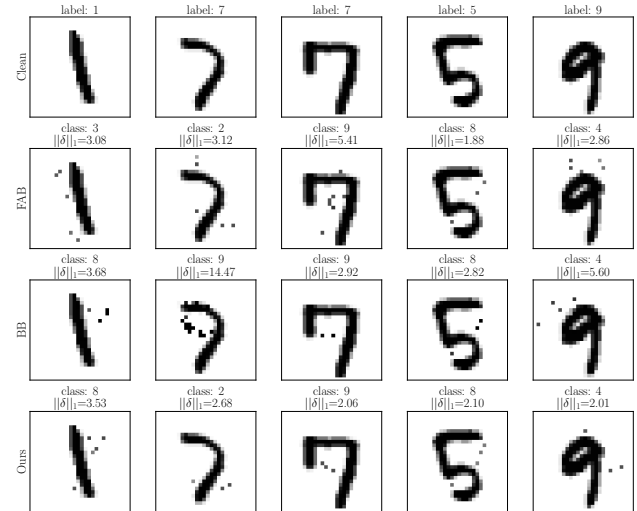


Figure 3. Untargeted ℓ_1 attacks against M2 (Madry et al., 2017).

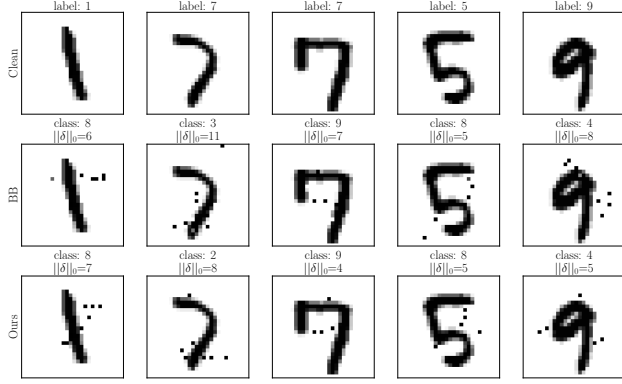


Figure 4. Untargeted ℓ_0 attacks against M2 (Madry et al., 2017).

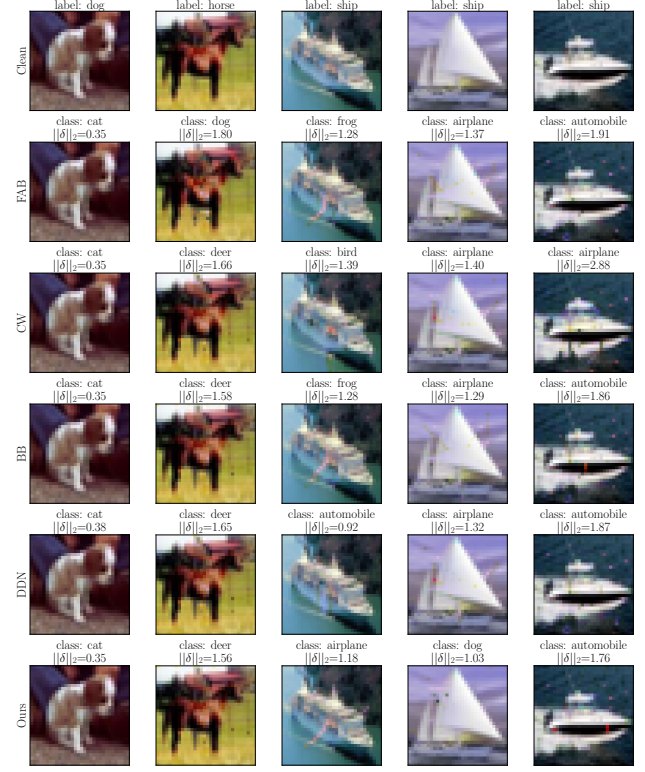


Figure 6. Untargeted ℓ_2 attacks against C2 (Carmon et al., 2019).



Figure 5. Untargeted ℓ_∞ attacks against C2 (Carmon et al., 2019).

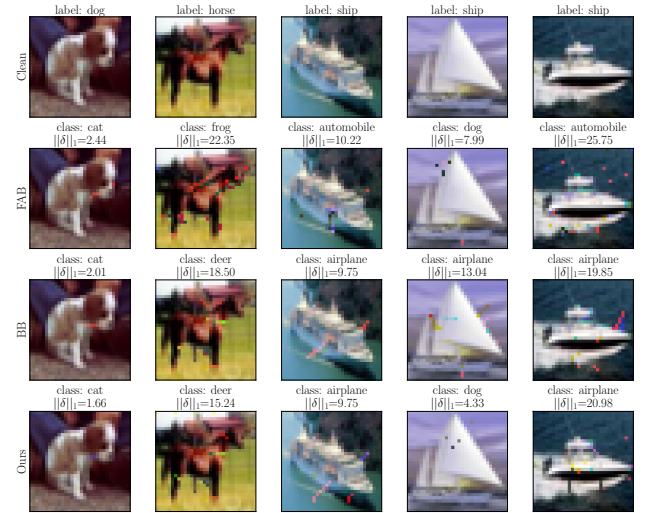


Figure 7. Untargeted ℓ_1 attacks against C2 (Carmon et al., 2019).

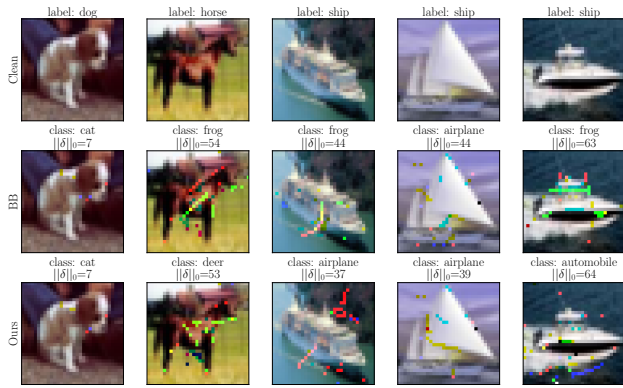


Figure 8. Untargeted ℓ_0 attacks against C2 (Carmon et al., 2019).

norms with fewer queries, with the exception of M2 (Figs. 9-10), where it seems to reach convergence more slowly than BB in ℓ_0 and ℓ_∞ . In ℓ_2 , the CW attack is the slowest to converge, due to the need of carefully tuning the weighting term, as described in Sect. 4.

On the CIFAR10 dataset (Figs. 11-12), our attack always rivals or outperforms the others, with the notable exception of DDN for the ℓ_2 norm, which sometimes finds smaller perturbations more quickly, as also shown in Table 3.

References

- Carmon, Y., Raghuathan, A., Schmidt, L., Duchi, J. C., and Liang, P. S. Unlabeled data improves adversarial robustness. In *Advances in Neural Information Processing Systems*, pp. 11192–11203, 2019.
- Madry, A., Makelov, A., Schmidt, L., Tsipras, D., and Vladu, A. Towards deep learning models resistant to adversarial attacks. *arXiv preprint arXiv:1706.06083*, 2017.

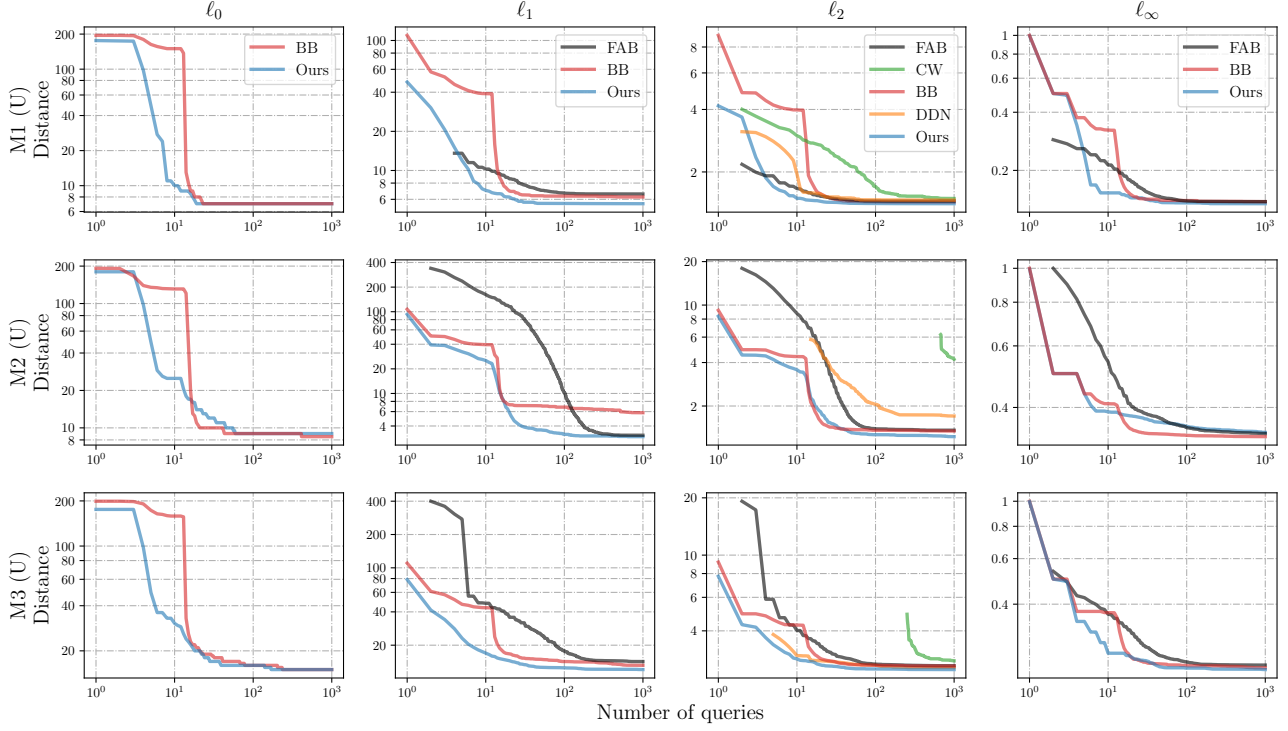


Figure 9. Query-distortion curves for untargeted (U) attacks on the M1 (top), M2 (middle), and M3 (bottom) MNIST models.

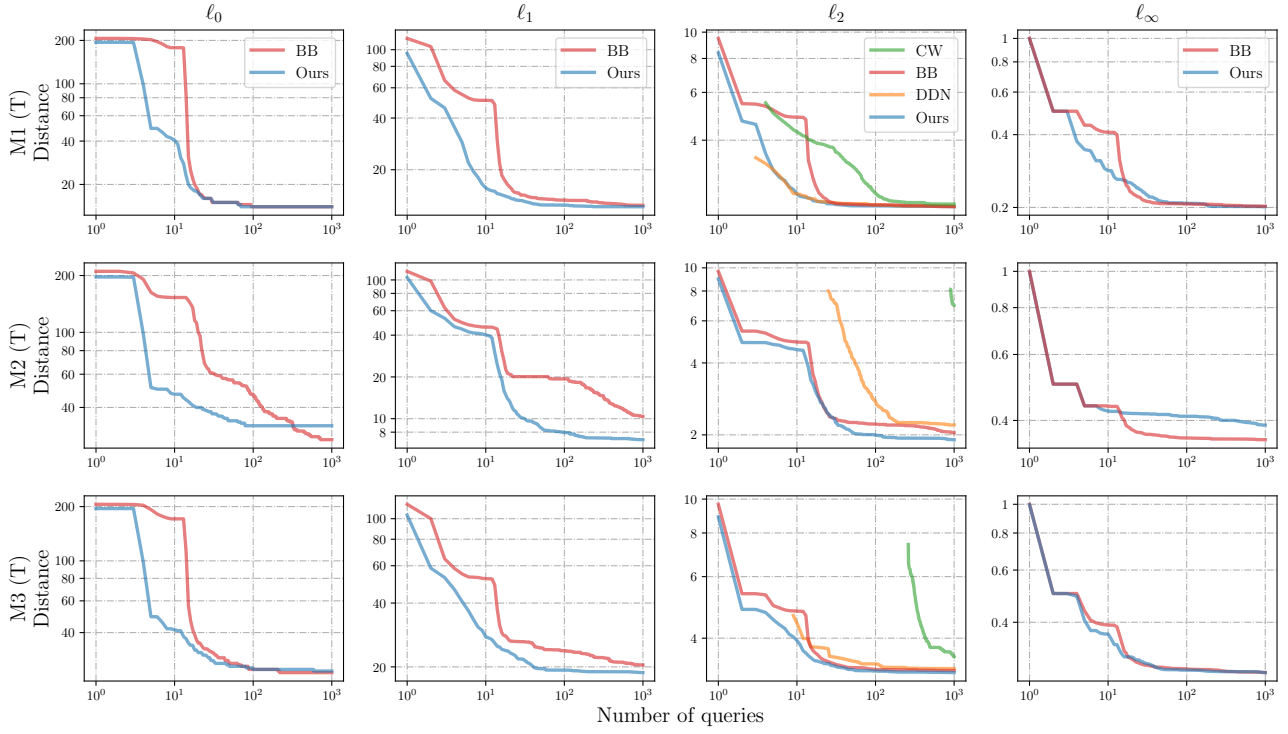


Figure 10. Query-distortion curves for targeted (T) attacks on the M1 (top), M2 (middle), and M3 (bottom) MNIST models.

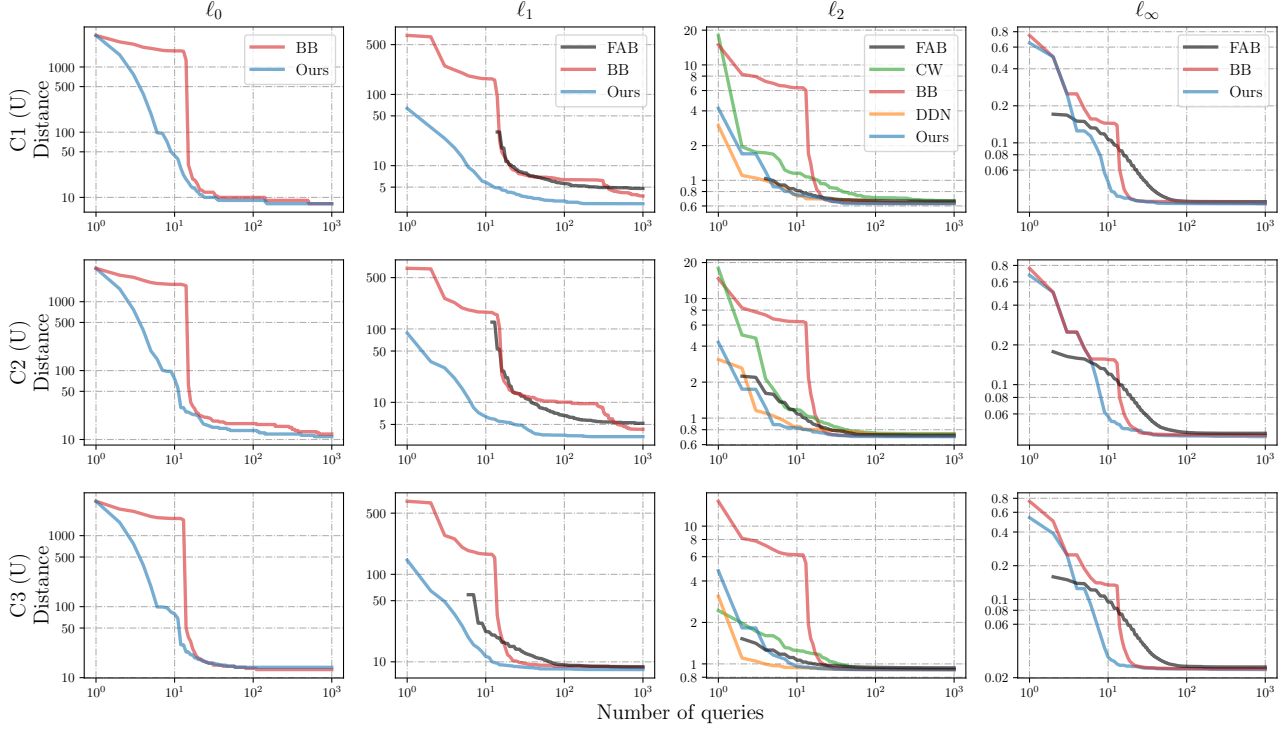


Figure 11. Query-distortion curves for untargeted (U) attacks on the C1 (top), C2 (middle), and C3 (bottom) CIFAR10 models.

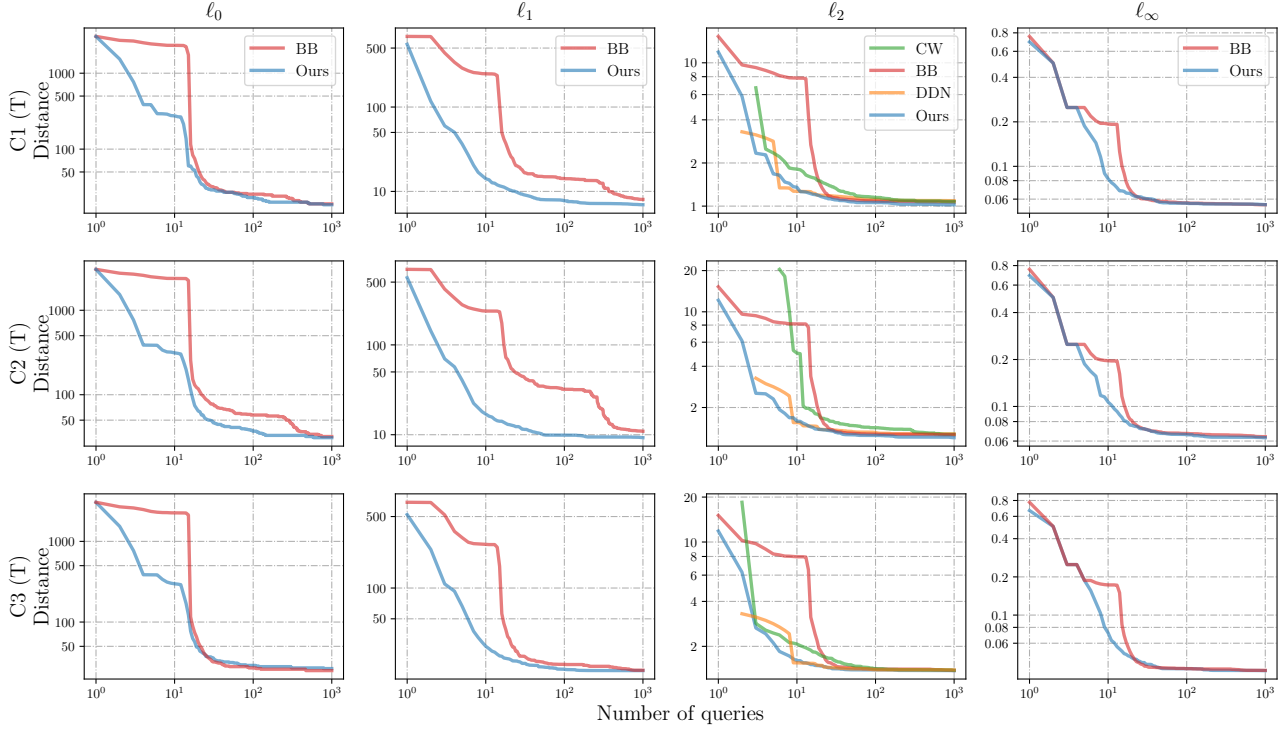


Figure 12. Query-distortion curves for targeted (T) attacks on the C1 (top), C2 (middle), and C3 (bottom) CIFAR10 models.